Discover Oncology

Research

TMCO1, as a potential biomarker of prognosis and immunotherapy response, regulates head and neck squamous cell carcinoma proliferation and migration

Ting Li[1] · Lu Chen[2] · Guangkai Zhou[1] · Yuhan Deng[3] · Meng Zhou[4] · Mingze Yan[1] · Shuyan Dong[1] · Kaixun Xing[1] · Shan Yu[2] · Hongjiang He[1]

Received: 5 January 2025 / Accepted: 18 April 2025
Published online: 01 May 2025

Abstract
Transmembrane and coiled-coil domains 1 (TMCO1), an endoplasmic reticulum transmembrane protein, actively regulates intracellular Ca^{2+} concentration and is associated with poor prognosis in several cancers. This study shows that TMCO1 is a potential biological prognostic indicator and therapeutic target for head and neck squamous cell carcinoma (HNSCC) by regulating the proliferation and migration of cancer cells, especially migration. We obtained TMCO1 expression data of HNSCC and normal tissues from The Cancer Genome Atlas (TCGA) and other databases and verified them with immunohistochemical staining. The results showed that high TMCO1 expression was significantly associated with HNSCC survival and tumor progression and was an independent prognostic factor for HNSCC. In addition, nomogram and receiver operating characteristic (ROC) curve, gene ontology, gene concentration and gene network analysis were used to reveal the function and regulatory mechanism of TMCO1. In vitro experiments confirmed that TMCO1 could promote proliferation, migration, invasion, adhesion and clonal formation of HNSCC cells. Furthermore, we analyzed the relationship between TMCO1 and tumor microenvironment, immune infiltration, immunotherapy and drug sensitivity, and found that patients with low TMCO1 expression were more suitable for immunotherapy, and suggested the selection of chemotherapy drugs. In conclusion, TMCO1 is a reliable biomarker in HNSCC, offering valuable guidance for clinical diagnosis and therapeutic strategies. These findings highlight its potential as a target for precision oncology in HNSCC.

Keywords HNSCC · TMCO1 · Prognosis · Biomarker · Immunotherapy

Ting Li and Lu Chen have contributed equally to the project.

Supplementary Information The online version contains supplementary material available at https://doi.org/10.1007/s12672-025-02437-y.

✉ Shan Yu, yushan@hrbmu.edu.cn; ✉ Hongjiang He, hehongjiang@ems.hrbmu.edu.cn; Ting Li, 2020021755@hrbmu.edu.cn; Lu Chen, chenlu_rong@126.com; Guangkai Zhou, zgk.8800@163.com; Yuhan Deng, 2020021711@hrbmu.edu.cn; Meng Zhou, zm18845765693@163.com; Mingze Yan, 2021021862@hrbmu.edu.cn; Shuyan Dong, 18304572241@163.com; Kaixun Xing, xingkashaun@163.com | [1]Department of Head and Neck Surgery, Harbin Medical University Cancer Hospital, No. 150 Haping Road, Nangang District, Harbin 150081, Heilongjiang, China. [2]Department of Pathology, Second Affiliated Hospital of Harbin Medical University, No. 246 XueFu Road, Harbin 150086, Heilongjiang, China. [3]Department of Breast Surgery, Harbin Medical University Cancer Hospital, No. 150 Haping Road, Nangang District, Harbin 150081, Heilongjiang, China. [4]Department of Anesthesiology, Harbin Medical University Cancer Hospital, No. 150 Haping Road, Nangang District, Harbin 150081, Heilongjiang, China.

Abbreviations

BP	Biological process
CC	Cellular component
COAD	Colon adenocarcinoma
CPTAC	Clinical proteomic tumor analysis consortium
CTLA4	Cytotoxic T lymphocyte antigen 4
ECM	Extracellular matrix
EMT	Epithelial-mesenchymal transition
GBM	Glioblastoma multiforme
GSEA	Gene set enrichment analysis
GO	Gene ontology
HNSCC	Head and neck squamous cell carcinoma
HPA	Human protein atlas
HR	Hazard ratio
IHC	Immunohistochemistry
IPS	Immune cell proportion score
KEGG	Kyoto Encyclopedia of Genes and Genomes
LSCC	Laryngeal squamous cell carcinoma
LUAD	Lung adenocarcinoma
MF	Molecular function
OS	Overall survival
OSCC	Oral squamous cell carcinoma
PBS	Phosphate buffered saline
PD1	Programmed death 1
PFS	Progression-free survival
R	Correlation coefficients
RFS	Recurrence free survival
ROC	Receiver operating characteristic
TCGA	The Cancer Genome Atlas
TME	Tumor microenvironment
TMCO1	Transmembrane and coiled-coil domains 1
UALCAN	The University of Alabama at Birmingham cancer data analysis portal
UBUC	Urinary bladder uroepithelial carcinoma

1 Introduction

Head and neck squamous cell carcinoma (HNSCC) ranks as the sixth most common cancer globally, with approximately 890,000 new cases and 450,000 deaths annually. This malignancy typically arises in the oral cavity, oropharynx, larynx, hypopharynx, or nasopharynx, and less frequently in the salivary glands or paranasal sinuses [1, 2]. Most patients are diagnosed with advanced stages (stages III and IV) [3]. Despite advancements in treatment modalities, including surgery, chemotherapy, radiotherapy, and immunotherapy, the prognosis for HNSCC remains dismal, with a 5-year overall survival (OS) rate below 60% [4]. Alarmingly, nearly 50% of patients with locally advanced HNSCC experience disease relapse or develop drug resistance following initial treatment, resulting in a median survival of approximately 12 months [5–8]. These statistics underscore the urgent need for reliable prognostic biomarkers and novel therapeutic targets to improve clinical outcomes in HNSCC.

TMCO1 has traditionally been studied in the context of genetic disorders, such as primary open-angle glaucoma and cerebro-facio-thoracic dysplasia, where its variants or mutations play a pathogenic role [9]. However, recent discoveries have unveiled TMCO1's function as a Ca^{2+} selective cation channel, with its knockdown leading to endoplasmic reticulum Ca^{2+} store overload, induction of apoptosis, and suppression of tumor growth [10, 11]. This tumor-suppressive role has been demonstrated in various cancers, including glioblastoma multiforme (GBM), lung adenocarcinoma (LUAD), colon adenocarcinoma (COAD), and urinary bladder uroepithelial carcinoma (UBUC) [12–16]. Despite these findings, the

mechanistic underpinnings of TMCO1 in cancer biology, particularly its potential as a prognostic biomarker or therapeutic target, remain underexplored.

Our study addressed this critical gap by investigating the role of TMCO1 in HNSCC, a context in which its function had not been previously elucidated. We revealed TMCO1 as a potential biological prognostic indicator and therapeutic target in HNSCC, demonstrating its ability to regulate cancer cell migration and adhesion. Furthermore, we comprehensively evaluated the association of TMCO1 expression with biological functions, the tumor microenvironment (TME), immune cell infiltration, immunotherapy response, and drug sensitivity. These analyses provided a holistic understanding of TMCO1's role in HNSCC progression and its potential clinical applications.

The novelty of our research lies in its multifaceted approach to unraveling TMCO1's significance in HNSCC. By integrating cellular-level experiments—including cell proliferation, scratch wound, invasion, adhesion, and colony formation assays—with broader analyses of the TME and immune landscape, we offer unprecedented insights into TMCO1's mechanistic contributions to HNSCC. Our findings not only expanded the current understanding of TMCO1's role in cancer biology but also highlight its potential as a biomarker for prognosis and a target for therapeutic intervention. This study paved the way for future research aimed at harnessing TMCO1's functional properties to develop innovative strategies for managing HNSCC, ultimately improving patient outcomes.

2 Materials and methods

2.1 Data source, tumor microarray and cell lines

The Cancer Genome Atlas (TCGA) database (https://portal.gdc.cancer.gov) provided the transcriptome profiling and clinical data of 504 HNSCC patients and 44 normal squamous epithelium. These data were used as a training cohort. The University of Alabama at Birmingham cancer data analysis portal (UALCAN) (http://ualcan.path.uab.edu/) was also used. This portal is an online tool. It provides access to the clinical proteomic tumor analysis consortium (CPTAC) database [17]. Most databases analyze gene expression at the mRNA level. CPTAC describes gene expression at the protein level. A total of 108 primary HNSCC and 71 normal epidermis samples were obtained from this database. The TCGA database was also accessed through the UALCAN online tool. Multiple validation was performed with 520 HNSCC samples and 44 normal epidermal samples from this database. Bioaitech provided 28 multisite HNSCC specimen tissues (HN810001) and seven multisite normal squamous epithelial tissues. These tissues were used as a validation cohort. Cal27, Tu212, and HW8 were cultured in 10%FBS + DMEM. They originated from tongue squamous cell carcinoma, laryngeal squamous cell carcinoma (LSCC), and oral squamous cell carcinoma (OSCC), respectively.

2.2 Immunohistochemistry (IHC) analysis

The human protein atlas (HPA) database (https://www.proteinatlas.org/) provided immunohistochemical images of esophageal squamous epithelium (id of Fig. 1E: 5236) and HNSCC (id of Fig. 1F: 4117; id of Fig. 1G: 2608; id of Fig. 1H: 4109).

The tissue microarray was baked and dewaxed in an oven at 67 °C. The sections were heated in boiling citrate buffer, then cooled and rinsed to block endogenous peroxidase activity. One drop of 3% H_2O_2 was added to each section, incubated for 10 min and rinsed. One drop of 1:500 primary antibody, polymer enhancer, enzyme-labeled anti-mouse/rabbit polymer (generic, Mysin), and freshly prepared DAB were applied to the sections, respectively. The sections were observed under the microscope for 5 min. Hematoxylin was used to restain the sections, which were differentiated in 0.1% HCl, rinsed in distilled water, and blued. The sections were dehydrated by gradient alcohol, cleared with xylene, sealed with neutral gum, and let dry for observation.

2.3 Survival and prognostic analysis

The "survminer" R package was used to perform Kaplan–Meier analysis of TMCO1 in the TCGA database. OS and progression-free survival (PFS) for high and low expression groups were obtained, using median values as thresholds. The Kaplan–Meier plotter database (http://kmplot.com) was used to estimate the effect of TMCO1 expression on HNSCC survival, with the median expression value as the default cutoff to define high and low expression groups. The hazard ratio (HR) with 95% confidence intervals and log-rank p value were displayed [18], and OS, PFS and recurrence free survival

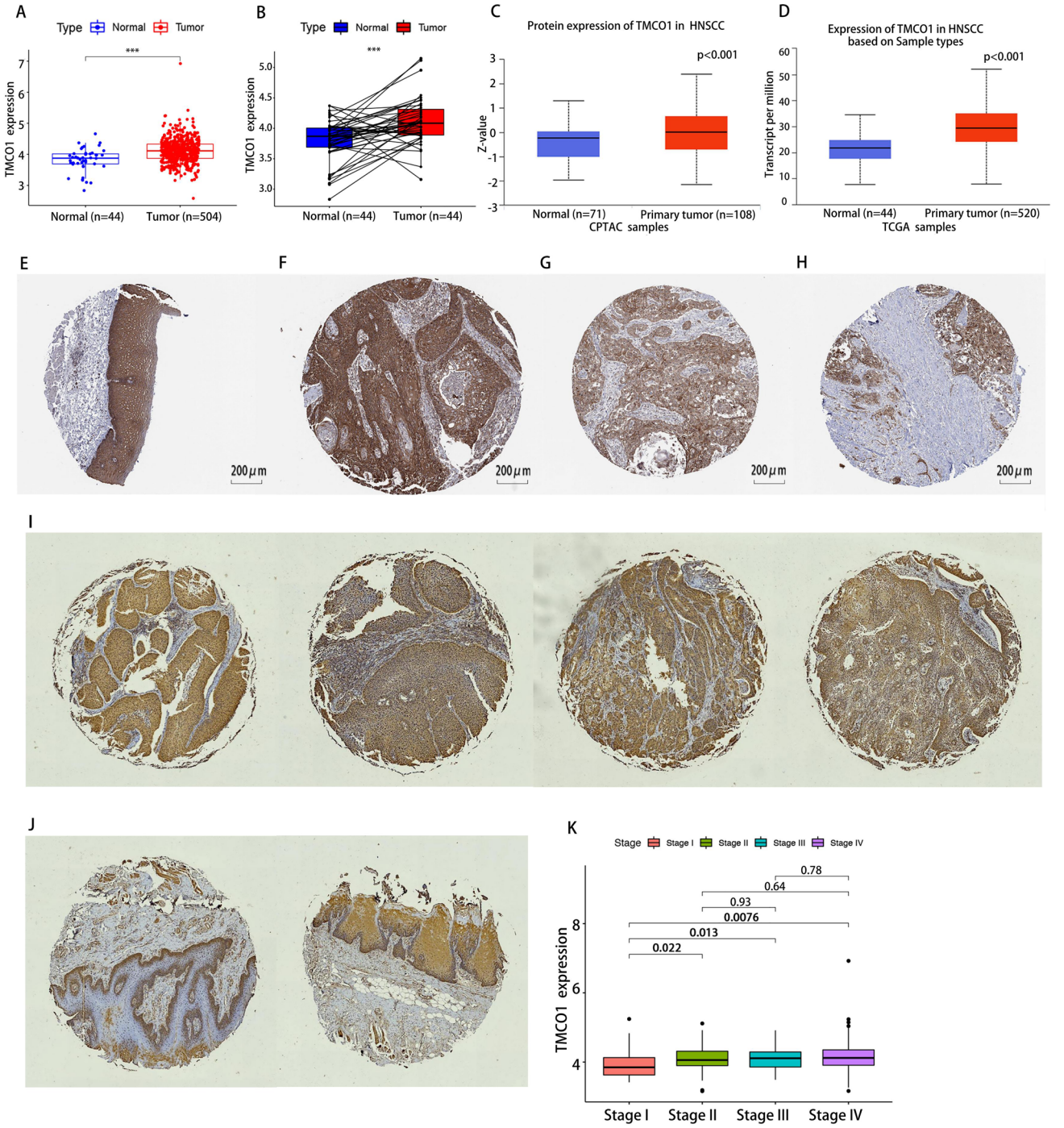

Fig. 1 TMCO1 expression is increased in HNSCC patients. **A** TMCO1 was overexpressed in HNSCC compared to normal squamous cells in the TCGA cohort. **B** In the TCGA cohort, TMCO1 was overexpressed in HNSCC compared to para-cancer tissue. **C**, **D** UALCAN accessed CPTAC and TCGA databases, and TMCO1 expression was significantly upregulated in HNSCC compared to normal squamous epithelial cells. **E** IHC images of TMCO1 protein in esophageal squamous epithelium in HPA database. **F**–**H** IHC image of TMCO1 protein in HNSCC tissue in HPA database. **I** IHC staining of TMCO1 protein in four representative multi-site HNSCC microarray tissue. **J** IHC staining of normal head and neck squamous epithelium in two representative multisite HNSCC microarray tissue. **K** Association of TMCO1 expression in the TCGA cohort between different stages of HNSCC. ***P < 0.001

(RFS) are calculated. Univariate Cox proportional hazards models were independently constructed for each candidate variable to estimate HR and p-values. All analyses were performed in separate R environments to ensure reproducibility. Subsequently, multivariate Cox analysis was conducted to assess the independent effects of variables after adjusting for potential confounders. Adjusted HRs and p-values were calculated, with multivariate analysis executed in an independent

R environment to prevent cross-contamination with univariate results. A nomogram model was developed to predict the 1-, 3-, and 5-year survival rates for HNSCC cases. A total score for each individual was calculated by summing up all the points, where a higher score indicated a higher risk of an event. Receiver operating characteristic (ROC) curves were used to assess the predictive accuracy of the model, where a larger AUC meant a better prediction accuracy.

2.4 Co-expression analysis

Co-expression analysis was performed on HNSCC data from the TCGA database. Genes that had co-expression relationships with TMCO1 were identified, using a corFilter = 0.6 and a pFilter = 0.001 as screening criteria. The genes with significant correlation coefficients (R) and P values were plotted in scatter plots. The "circlize" R package was also used to screen the core genes related to TMCO1 and to predict the gene regulatory network.

2.5 Differential gene analysis

The 50 most significant upregulated and downregulated genes related to TMCO1 in HNSCC data from the TCGA database were displayed by the "pheatmap" R package, using a logFCfilter = 1 and an fdrFilter = 0.05 as filters. Pseudogenes that had lost normal functional DNA sequences were excluded.

2.6 Functional and pathway analysis

The R package "Org.Hs.eg.db" was used to perform gene ontology (GO), Kyoto Encyclopedia of Genes and Genomes (KEGG), and gene set enrichment analysis (GSEA) on HNSCC data from the TCGA database. A logfcfilter = 1 and an fdrfilter = 0.05 were applied as filtering criteria.

2.7 Adhesion assay

Two groups were divided for each cell line: a control group and an overexpression group. The same cell lines and groups were used for further cell experiments. The culture plates were coated with LN, FN, type I collagen and Lys, which are the main components of the extracellular matrix (ECM). Each well of a 96-well plate was added with 100ul of coating solution. The plate was soaked with BSA and culture medium. The cells were trypsinized, washed and re-suspended in culture medium. The cells were counted and $5*10^4$ cells were seeded in each well of the pre-treated 96-well plate. The plate was incubated at 37℃ in a 5% CO2 incubator for 1 h to allow the cells to adhere to the monolayer. After washing, the remaining cells attached to the monolayer were observed and counted under a microscope.

2.8 Wound healing assay

The cells were cultured to logarithmic growth phase and $5*10^5$ cells per well were seeded in 6-well plates. They were incubated at 37 °C and 5% CO_2 until they reached confluence. A vertical scratch on the cell monolayer was made by a 200ul pipette tip. The cells were washed with phosphate buffered saline (PBS) and serum-free medium was added. The position and width of the scratches were recorded under a microscope at 0 h. The cells were incubated for another 24 h and photographed under a microscope to measure the migration distance.

2.9 Migration assay

The same cell lines and groups as described above were used. Matrigel was diluted with serum-free medium or PBS at a 1:8 ratio at 4 ℃ and 100 µl was coated on the upper chamber of Transwell inserts. They were incubated at 37 ℃ overnight to solidify. Cell suspension with a density of $5*10^5$/mL was prepared and 500 µL of serum-containing medium was added to the lower chamber of 24-well plates. The Transwell inserts were placed in the plates with tweezers and 200µL of cell suspension per well was added to the upper chamber. They were incubated at 37 °C and 5% CO_2 for 24 h. When the cells migrated to the lower chamber, the Matrigel and the cells in the upper chamber were gently removed with a cotton swab. The cells were fixed and stained with 4% paraformaldehyde and 0.5% crystal violet, respectively. They were observed and photographed under a microscope. Ten fields per well were randomly selected and counted and the average value was calculated.

2.10 Cell proliferation assay

Cell viability was measured by the CCK-8 kit from Biotime company. 2000 cells per well were seeded in 96-well plates with six replicates for each time point and 100 µl of culture medium per well. The plates were surrounded with PBS buffer to prevent evaporation and incubated at 37 ℃ and 5% CO_2 for different durations. 10 µL of CCK-8 reagent was added to each well and incubated for an optimal time determined by a pre-experiment. The absorbance at 450 nm was read using a microplate reader.

2.11 Colony formation assay

The same cell lines and groups as described above were used. The cells in logarithmic growth phase were digested with trypsin, resuspended in 2X1640 medium containing 20% FBS and 2X antibiotics, and counted. Low melting point agarose solutions (1.2% and 0.7%) were autoclaved and kept in a 55 °C water bath. The bottom layer gel was made by mixing the 1.2% agarose solution with 2X medium at a 1:1 ratio. Each well of a 6-well plate was added with 1.5 mL of the mixture, and solidified at room temperature. The cell density was adjusted to $5*10^4$/mL, and the top layer gel was made by mixing the 0.7% agarose solution with 2X medium at a 1:1 ratio. Each well was added with 100 µL of cell suspension (5,000 cells), and mixed well. The plate was incubated at 37 °C, 5% CO_2 and saturated humidity for 15 days, and the medium was replenished every three days. After washing with PBS, the cells were fixed with 4% paraformaldehyde and stained with crystal violet. The clones were photographed by digital camera, and the number of clones in each well was counted and compared between the control group and the OE group. The cloning efficiency was calculated.

2.12 Correlation of tumor immune cell infiltration

The immune score, stromal score, and ESTIMATE score (the sum of immune and stromal scores) of the HNSCC samples from the TCGA database were calculated by the ESTIMATE algorithm to analyze the variance of TME. The CIBERSORT method with pFilter = 0.05 was applied to determine the type and distribution of various immune cells in HNSCC. 22 types of TIICs were identified based on their correlation and differential expression levels with TMCO1. The correlation between TMCO1 and immune checkpoint-related genes was also analyzed using pFilter = 0.001 as the p-value threshold for the correlation test.

2.13 Immunotherapy prediction

The effect of anti programmed death 1 (PD1) and anti cytotoxic T lymphocyte antigen 4 (CTLA4) immunotherapy between the high and low TMCO1 expression groups was compared based on TMCO1 expression in the TCGA cohort. The immune cell proportion score (IPS) was used as a criterion to identify the groups that benefited from immunotherapy.

2.14 Drug sensitivity prediction

The IC50 of HNSCC patients was estimated by the "pRRophetic" R package to evaluate the effect of TMCO1 on chemotherapeutic sensitivity. IC50 is the drug or substance concentration that inhibits a biological process (or a component of that process, such as an enzyme, cell receptor, or microorganism) by 50%.

2.15 Statistics analysis

R 4.2.1 software (https://www.rproject.org/) and SPSS software (Version 23.0; IBM, Armonk, NY, USA) were used for all statistical analyses. $P < 0.05$ was considered statistically significant.

3 Results

3.1 TMCO1 overexpression in HNSCC

TMCO1 expression was significantly elevated in HNSCC at both RNA and protein levels. TMCO1 RNA expression was markedly higher in HNSCC patients (n = 504) than in normal squamous epithelium (n = 44) according to TCGA data

(Fig. 1A, ***P < 0.001), and the same result was shown by paired difference analysis (P < 0.001, Fig. 1B). The increased protein expression of TMCO1 in HNSCC was demonstrated by CPTAC and HPA databases as well as IHC staining data of tissue microarray. Higher TMCO1 protein expression was detected in CPTAC database (108 HNSCC vs 71 normal, P < 0.001, Fig. 1C). TMCO1 expression was markedly elevated in TCGA samples consisting of 520 HNSCC patients and 44 normal samples (P < 0.001, Fig. 1D). The HPA database showed that TMCO1 protein expression was higher in HNSCC tissues (Fig. 1F–H) than in normal esophageal squamous epithelium (Fig. 1E), with high levels of quantity > 75%, strong intensity and high antibody staining. The tissue microarray HN810001 showed that TMCO1 protein level was significantly increased in HNSCC tissues, 19 cases were strongly stained, 4 cases were moderately stained, and 5 cases were weakly stained. Representative images of HNSCC (Fig. 1I) and normal head and neck squamous epithelium (Fig. 1J) were selected to illustrate these findings.

Further clinical correlation analysis revealed that TMCO1 expression in HNSCC patients increased significantly after stage I, with statistically distinct differences compared to stages II, III, and IV (P = 0.022 between I and II, P = 0.013 between I and III, and P = 0.0076 between I and IV) (Fig. 1K). No significant association was observed between TMCO1 expression and stages II, III, or IV, suggesting that TMCO1 expression is primarily linked to the early stages of HNSCC.

3.2 TMCO1 expression as a prognostic marker in HNSCC

TMCO1 expression was significantly associated with poorer survival outcomes in HNSCC patients. Analysis of the TCGA cohort (n = 504) revealed that high TMCO1 expression was negatively correlated with OS (Fig. 2A, P < 0.001), PFS (Fig. 2B, P < 0.001) and RFS (supplementary figure, P = 0.013). These findings were further validated using the Kaplan–Meier Plotter database, which showed that patients with high TMCO1 expression (n = 269) had significantly worse OS compared to those with low TMCO1 expression (n = 230) (Fig. 2C, logrank P = 5.2e−07). Similarly, high TMCO1 expression (n = 58) was associated with shorter PFS than low TMCO1 expression (n = 66) (Fig. 2D, logrank P = 0.013).

Univariate Cox analysis of the TCGA cohort (n = 504) identified TMCO1 (HR = 1.989; P < 0.001), age (HR = 1.024; P < 0.001), and stage (HR = 1.451; P < 0.001) as significant prognostic factors for HNSCC (Fig. 2E). Multivariate Cox analysis further confirmed that TMCO1 (HR = 1.877; P < 0.001), age (HR = 1.026; P < 0.001), and stage (HR = 1.479; P < 0.001) were independent predictors of survival, regardless of other clinical traits (Fig. 2F).

3.3 TMCO1 co-expression analysis in HNSCC

To explore the regulatory network of TMCO1 in HNSCC, we analyzed co-expressed genes using data from the TCGA database (n = 504). The analysis identified TIPRL (Fig. 3A, R = 0.73, P < 0.001), C1orf43 (Fig. 3B, R = 0.62, P < 0.001), ODR4 (Fig. 3C, R = 0.61, P < 0.001), and SDHC (Fig. 3D, R = 0.73, P < 0.001) as significantly co-expressed with TMCO1.

The co-expression relationships were further visualized using a circle plot (Fig. 3E). The plot revealed that SRP9, PEX19, SDHC, ODR4, C1orf43, and TIPRL were positively regulated by TMCO1 (red connections), while MAP4, USP2, MYO1G, EHBP1L1, and KIF1C were negatively regulated (green connections).

3.4 TMCO1 differential gene analysis in HNSCC

To further explore the biological roles of TMCO1, GO and KEGG enrichment analyses were performed using transcriptomic data from TCGA HNSCC (n = 504), with a p-value cutoff of 0.05.

The bar chart (Fig. 4A) highlighted the top 10 significant terms in biological process (BP), cellular component (CC), and molecular function (MF) categories. TMCO1 was notably involved in keratinization-related processes, including keratinization (P = 1.11e−15) and keratinocyte differentiation (P = 4.37e−13) in the BP group. In the CC group, TMCO1 was enriched in keratin filaments (P = 2.03e−05), intermediate filaments (P = 2.45e−05), and intermediate filament cytoskeleton (P = 8.36e−05). Additionally, TMCO1 correlated with the activity of anion transmembrane channels, such as chloride channels (P = 8.07e−05), in the MF group.

KEGG analysis revealed that TMCO1 was associated with platinum resistance (P = 0.049), tyrosine metabolism (P = 0.013), and glutathione metabolism (P = 0.031), further supporting its role in platinum resistance (Fig. 4B).

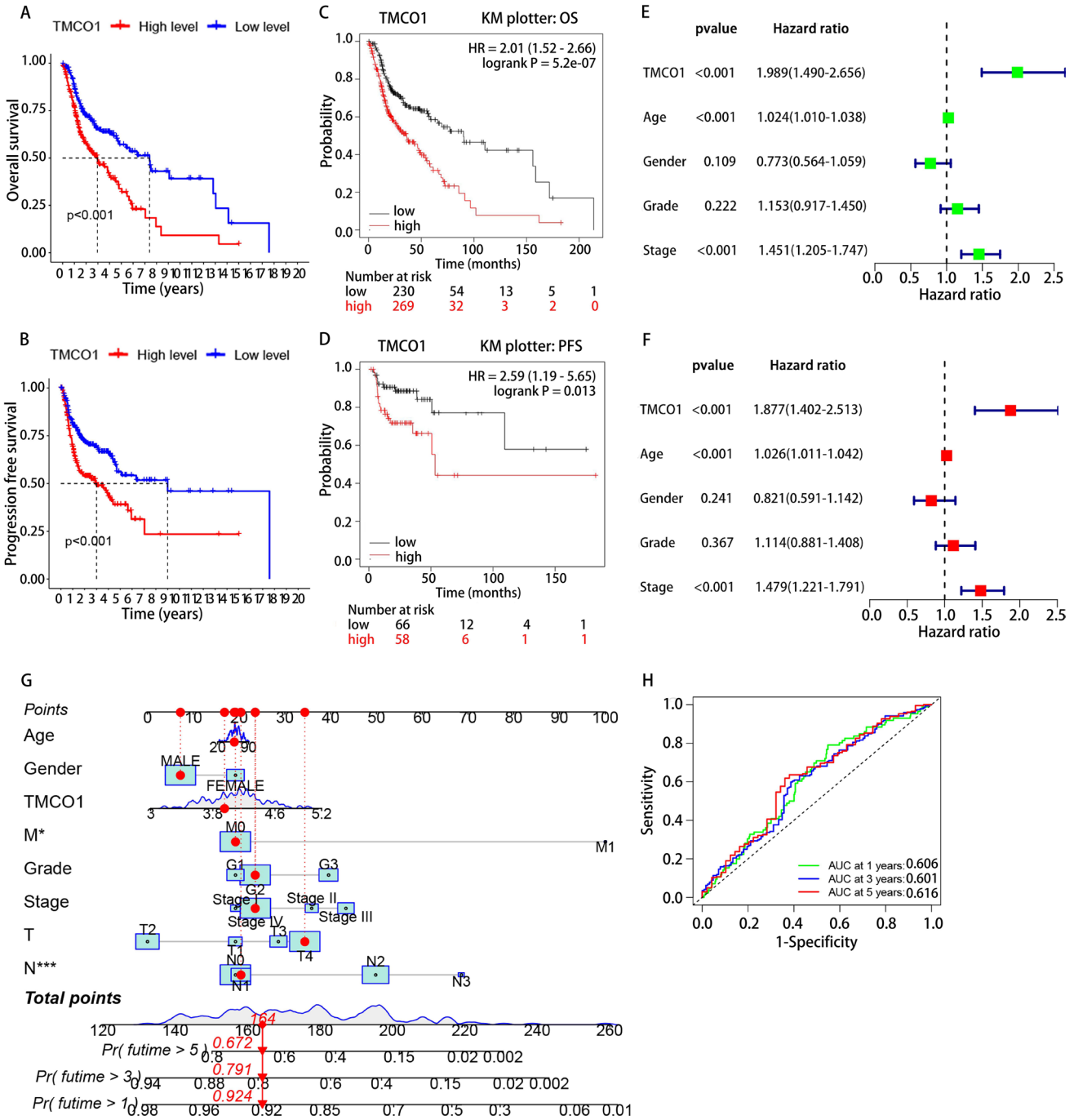

Fig. 2 TMCO1 is a poor prognostic marker of HNSCC. **A**, **B** In HNSCC samples from the TCGA cohort (Median as cutoff), the OS and PFS of the group with high TMCO1 expression was significantly down-regulated. **C**, **D** In Kaplan–Meier plotter (Median as cutoff), HNSCC patients with high TMCO1 expression had worse OS and PFS than those with low expression. **E**, **F** In univariate (green) and multivariate (red) analysis of HNSCC samples in the TCGA cohort, TMCO1 expression, age and stage were important prognostic factors. **G** Nomogram for predicting 1-, 3-, and 5-year OS about TMCO1 of TCGA cohort in the HNSCC sample. **H** Time-dependent ROC curves of TMCO1 on HNSCC from the TCGA cohort. $P < 0.001$

GSEA (Fig. 4C) demonstrated that drug metabolism cytochrome P450 and metabolism of xenobiotics by cytochrome P450 were significantly enriched in the high TMCO1 expression group. In contrast, allograft rejection, ECM-receptor interaction, and viral myocarditis were enriched in the low TMCO1 expression group.

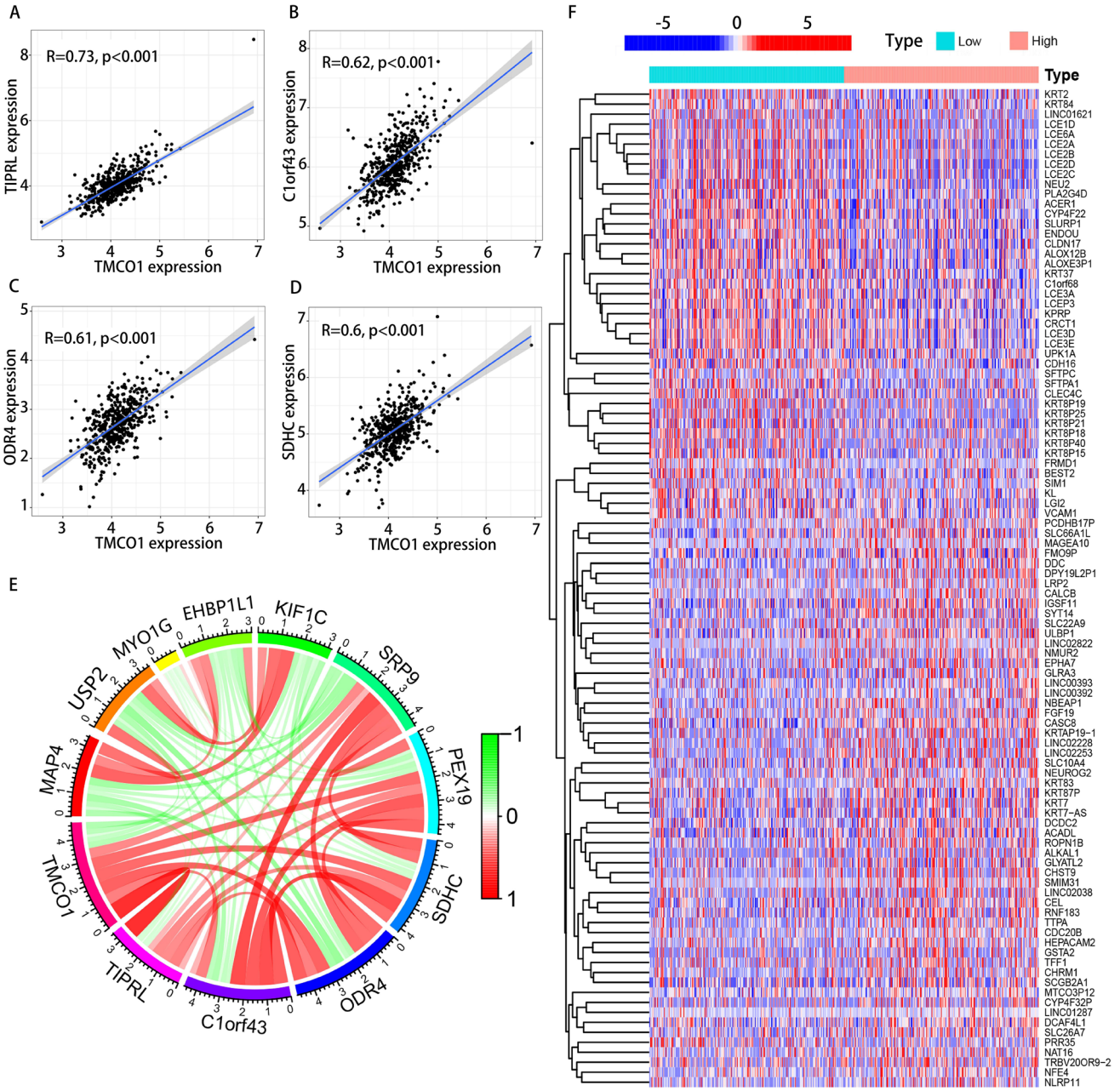

Fig. 3 Genes associated with TMCO1. **A**–**D** TIPRL, C1orf43, ODR4 and SDHC were the co-expressed genes of TMCO1 in HNSCC patients in the TCGA cohort. **E** Co-expression circle plot of TMCO1 in the TCGA cohort from HNSCC. **F** Divide HNSCC samples from TCGA queue into two groups based on TMCO1 expression median. Express the top 50 upregulated and downregulated genes as a heatmap. $P < 0.001$

3.5 Promotion of adhesion, migration, invasion, proliferation and clonal formation of HNSCC cells in vitro by TMCO1

ECM adhesion assays revealed that TMCO1 overexpression significantly increased the adhesion of Cal27, Tu212, and HW8 cells to four ECM components: laminin (LN), fibronectin (FN), collagen I, and lysine (Lys) (Fig. 5A). Cells in the overexpressed group appeared flatter, more clustered, and darker compared to the control group, indicating stronger adhesion capabilities.

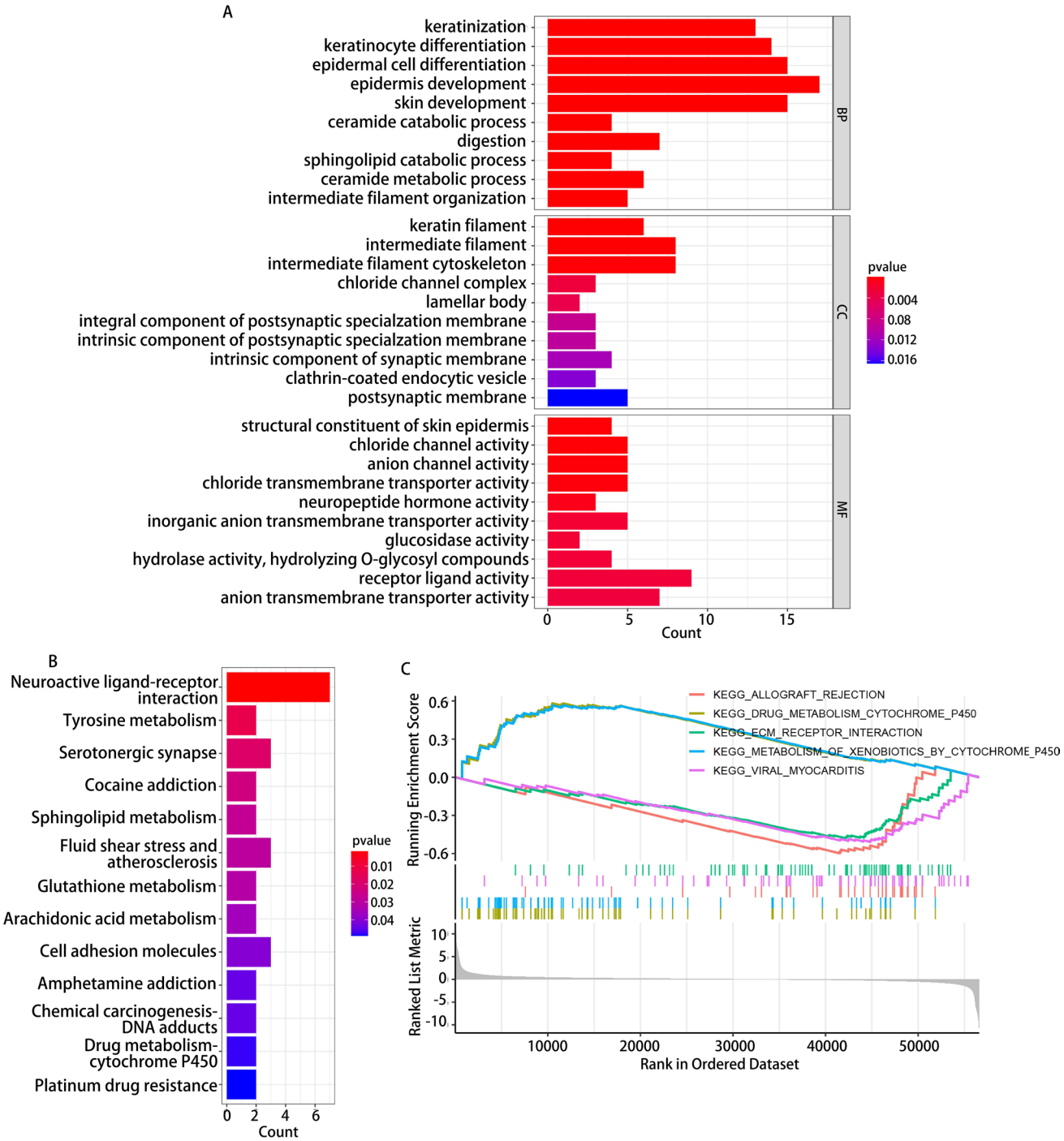

Fig. 4 Functional enrichments of TMCO1 in HNSCC. **A** GO enrichment analysis of TMCO1 on HNSCC from the TCGA cohort. **B** KEGG enrichment analysis regarding of TMCO1 in TCGA samples from HNSCC. **C** GSEA analysis about TMCO1 of TCGA cohort in the HNSCC sample

Wound healing assays demonstrated that TMCO1 overexpression enhanced the migration ability of all tested cell lines (Fig. 5B–D). After 24 h, the scratch area in the overexpressed group showed increased cell density and tightly arranged cells, forming a stable cell layer. These results suggest that TMCO1 positively regulates cell migration in HNSCC.

Matrigel invasion assays further confirmed that TMCO1 overexpression enhanced the invasive potential of HNSCC cells (Fig. 5E). The overexpressed group exhibited higher cell density and darker staining, indicating stronger penetration and invasion abilities compared to the control group.

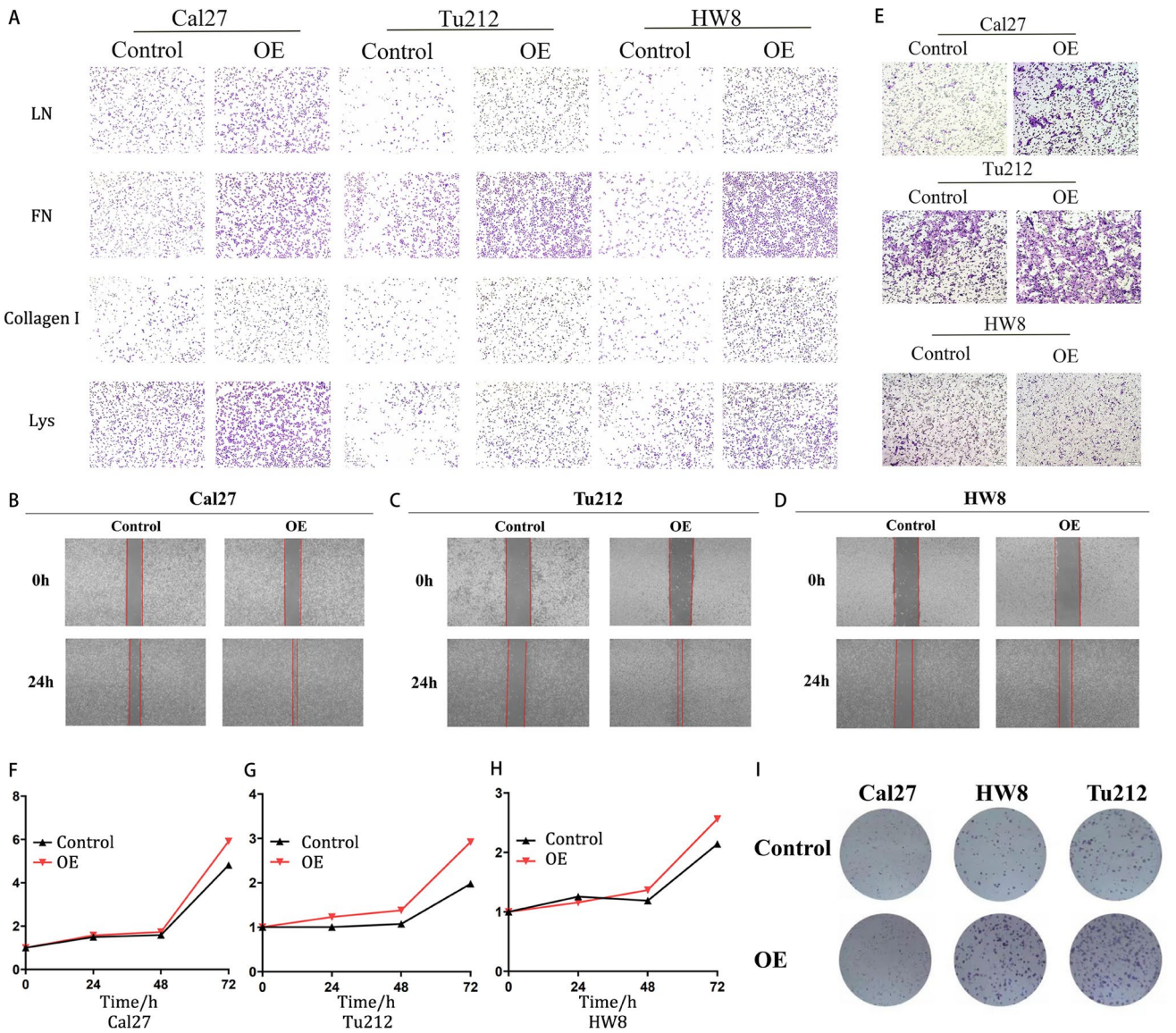

Fig. 5 Phenotypic study of HNSCC malignization by overexpression of TMCO1. **A** In the adhesion assay, overexpression of TMCO1 could enhance the adhesion of HNSCC cell lines Cal27, Tu212 and HW8 cells to LN, FN, Collagen I and Lys. **B**–**D** Among the three HNSCC cell lines in the wound healing assay, the migration ability of the overexpression group of TMCO1 was higher than that of the control group, and the cell density in the 24 h scratch area was further increased. **E** In the invasion assay of three HNSCC cell lines, the invasion of Matrigel coating in the overexpression group of TMCO1 was higher than that in the control group. **F**–**H** In all HNSCC cell lines, the cell viability and proliferation ability of overexpression group of TMCO1 were higher than that of control group after 48 h. **I** In the clonal formation assay of the three groups of cells, the proliferation of HNSCC cell lines overexpressing TMCO1 was higher

Cell proliferation assays revealed that TMCO1 overexpression significantly increased the viability and proliferation ability of Cal27, Tu212, and HW8 cells after 48 h (Fig. 5F–H). These findings suggest that TMCO1 may play a role in promoting cell proliferation in HNSCC.

Soft agar clonal formation assays showed that HNSCC cell lines overexpressing TMCO1 exhibited higher proliferative and malignant potential (Fig. 5I). The overexpressed group formed more and larger colonies, further supporting the role of TMCO1 in enhancing tumorigenic properties.

Fig. 6 TMCO1 Modulates Immune Infiltration in HNSCC. **A** Higher TME scores in the TCGA cohort of HNSCC patients with TMCO1 low ▶ expression. **B** Immune cell differential analysis of TMCO1 using CIBERSORT. **C** Correlation analysis of immune cells in HNSCC samples from the TCGA cohort. **D** Correlation of TMCO1 expression with some immune checkpoints in HNSCC. **E** Low TMCO1 expression in HNSCC samples from TCGA was associated with higher IPS when treated with anti-PD-1 therapy. **F** High TMCO1 expression in HNSCC samples from TCGA was associated with higher IPS when treated with anti-CTLA4 therapy. **G** Low TMCO1 expression in HNSCC samples from TCGA is associated with higher IPS when treated with anti-PD-1 and anti-CTLA4 combination therapy. **H** Low TMCO1 expression in HNSCC samples from TCGA is associated with higher IPS scores when not treated with anti-PD-1 and anti-CTLA4 therapy. *P < 0.05; **P < 0.01; ***P < 0.001

3.6 TMCO1 expression predicts immunotherapy response in HNSCC

To evaluate the potential role of TMCO1 in immunotherapy response, we analyzed the transcriptome data of TCGA HNSCC (n = 504) using IPS as a metric. IPS scores were calculated under different treatment conditions, including anti-PD1 alone, anti-CTLA4 alone, combined anti-PD1 and anti-CTLA4, and no treatment.

The results showed that the low TMCO1 expression group had significantly higher IPS scores compared to the high expression group when treated with anti-PD1 alone (Fig. 6E, P = 0.0043). Similarly, in the combined treatment of anti-PD1 and anti-CTLA4, the low TMCO1 expression group also exhibited higher IPS scores (Fig. 6G, P = 0.0074). These findings suggest that low TMCO1 expression is associated with a better response to anti-PD1 therapy, regardless of whether anti-CTLA4 is included. In contrast, no significant difference in IPS scores was observed between the high and low TMCO1 expression groups when treated with anti-CTLA4 alone (Fig. 6F) or without any drug (Fig. 6H). This indicates that anti-CTLA4 treatment does not influence the response of TMCO1 in HNSCC patients.

3.7 Drug sensitivity prediction of TMCO1 in HNSCC

By analyzing the data mining cohort (n = 504) of HNSCC in the TCGA database, 31 box plots with statistical significance were obtained (Fig. 7A–X, Fig. 8A–G). Among them, 24 drugs were more sensitive in the high TMCO1 expression group, including A-443654 (Fig. 7A, P = 3e−05), AKT inhibitor VIII (Fig. 7B, P = 1.6e−06), AZ628 (Fig. 7C, P = 4.4e−07), BI-2536 (Fig. 7D, P = 0.00057), Docetaxel (Fig. 7E, P = 2.1e−05), FH535 (Fig. 7F, P = 7.3e−09), FK866 (Fig. 7G, P = 0.00035), GW 441756 (Fig. 7H, P = 1.6e−05), GW843682X (Fig. 7I, P = 0.00099), IOX2 (Fig. 7J, P = 0.00031), JNK-9L (Fig. 7K, P = 0.00015), KIN001-266 (Fig. 7L, P = 0.00012), Masitinib (Fig. 7M, P = 0.00036), Mitomycin C (Fig. 7N, P = 0.00096), MLN4924 (Fig. 7O, P = 6.2e−05), MS-275 (Fig. 7P, P = 8.5e−05), Pyrimethamine (Fig. 7Q, P = 8.6e−07), Roscovitine (Fig. 7R, P = 0.00098), Salubrinal (Fig. 7S, P= 6.5e−05), SB52334 (Fig. 7T, P = 0.00018), Sorafenib (Fig. 7U, P = 0.00015), Thapsigargin (Fig. 7V, P = 0.00077), Tipifarnib (Fig. 7W, P = 9.4e−05), and Vinorelbine (Fig. 7X, P = 3.6e−06).

The following 7 drugs were more drug-sensitive in the low TMCO1 expression group: AMG-706 (Fig. 8A, P = 0.00073), Cyclopamine (Fig. 8B, P = 0.00065), Navitoclax (Fig. 8C, P = 7.5e−08), NU-7441 (Fig. 8D, P = 0.00057), Saracatinib (Fig. 8E, P = 0.00033), WZ-1–84 (Fig. 8F, P = 3.1e−05), and XL-184 (Fig. 8G, P = 0.00076).

4 Discussion

Through bioinformatics analysis and in vitro experiments, we identified TMCO1 as a highly expressed oncogene in HNSCC, serving as a potential biomarker and therapeutic target associated with poor prognosis and aggressive cancer phenotypes. While TMCO1 exhibits oncogenic roles in GBM, LUAD, and COAD, its tumor-suppressive function in UBUC suggests tissue-specific heterogeneity, underscoring the complexity of its biological functions [12, 13, 15, 16]. Our study corroborates and expands the association of TMCO1 with HNSCC prognosis and immunotherapy response. This is the first comprehensive study of TMCO1 in HNSCC.

TMCO1 expression levels inversely correlated with survival, consistent with Li et al. [19]. However, our study extended beyond this observation by systematically evaluating TMCO1's multifaceted impact on HNSCC progression. TMCO1 expression was significantly associated with tumor stage, with stage I showing distinct differences compared to stages II-IV, suggesting its potential role in early HNSCC onset. This aligns with its function in LUAD [13], yet contrasts with its association with advanced stages in COAD [12], highlighting the need for further validation in

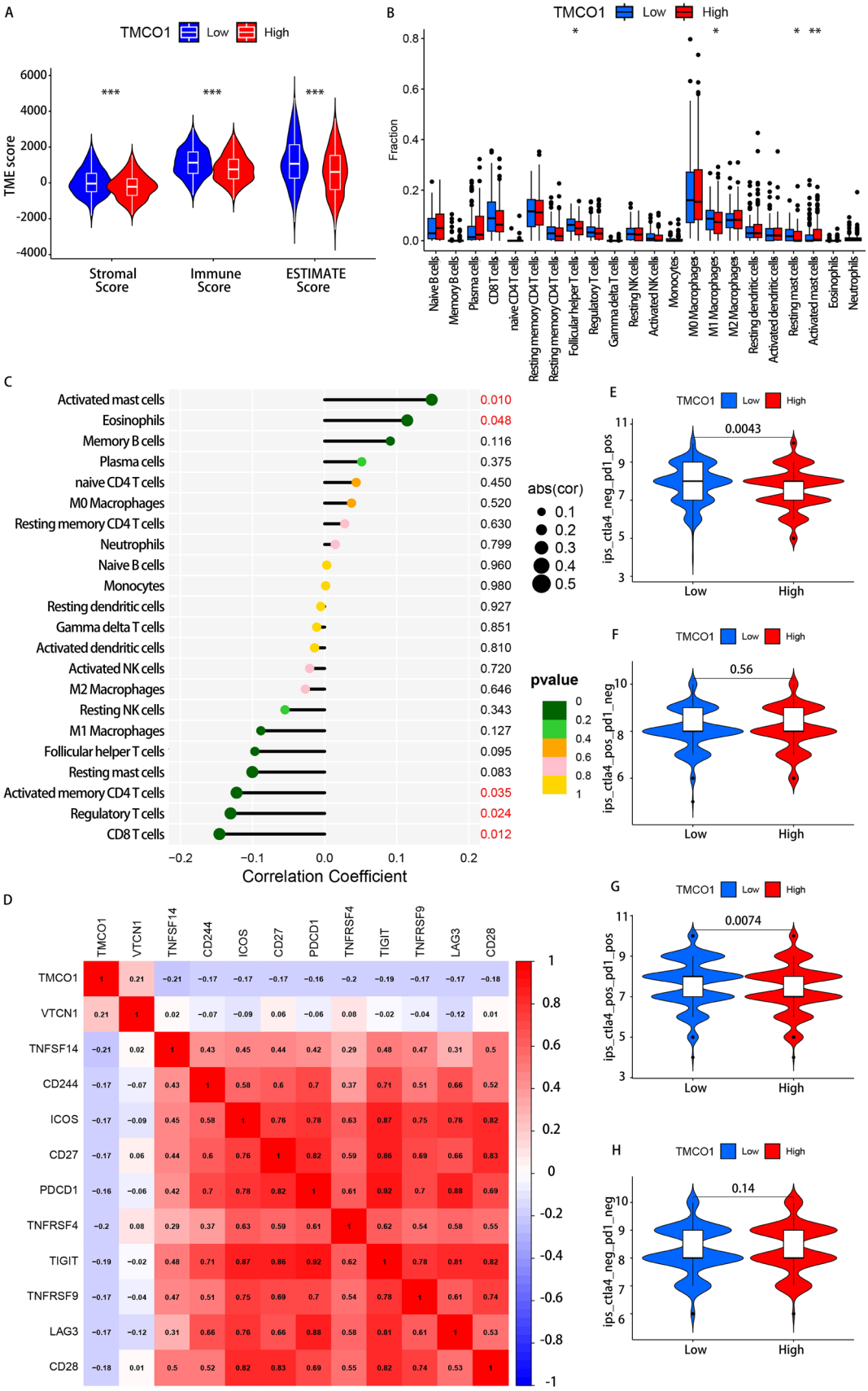
A
TMCO1 Low High
TME score
Stromal Score
Immune Score
ESTIMATE Score
B
TMCO1 Low High
Fraction
Naive B cells
Memory B cells
Plasma cells
CD8 T cells
naive CD4 T cells
Resting memory CD4 T cells
Follicular helper T cells
Regulatory T cells
Gamma delta T cells
Resting NK cells
Activated NK cells
Monocytes
M0 Macrophages
M1 Macrophages
M2 Macrophages
Resting dendritic cells
Activated dendritic cells
Resting mast cells
Activated mast cells
Eosinophils
Neutrophils
C
Activated mast cells 0.010
Eosinophils 0.048
Memory B cells 0.116
Plasma cells 0.375
naive CD4 T cells 0.450
M0 Macrophages 0.520
Resting memory CD4 T cells 0.630
Neutrophils 0.799
Naive B cells 0.960
Monocytes 0.980
Resting dendritic cells 0.927
Gamma delta T cells 0.851
Activated dendritic cells 0.810
Activated NK cells 0.720
M2 Macrophages 0.646
Resting NK cells 0.343
M1 Macrophages 0.127
Follicular helper T cells 0.095
Resting mast cells 0.083
Activated memory CD4 T cells 0.035
Regulatory T cells 0.024
CD8 T cells 0.012
Correlation Coefficient
abs(cor)
pvalue
D
TMCO1 VTCN1 TNFSF14 CD244 ICOS CD27 PDCD1 TNFRSF4 TIGIT TNFRSF9 LAG3 CD28
E
TMCO1 Low High
0.0043
ips_ctla4_neg_pd1_pos
F
TMCO1 Low High
0.56
ips_ctla4_pos_pd1_neg
G
TMCO1 Low High
0.0074
ips_ctla4_pos_pd1_pos
H
TMCO1 Low High
0.14
ips_ctla4_neg_pd1_neg

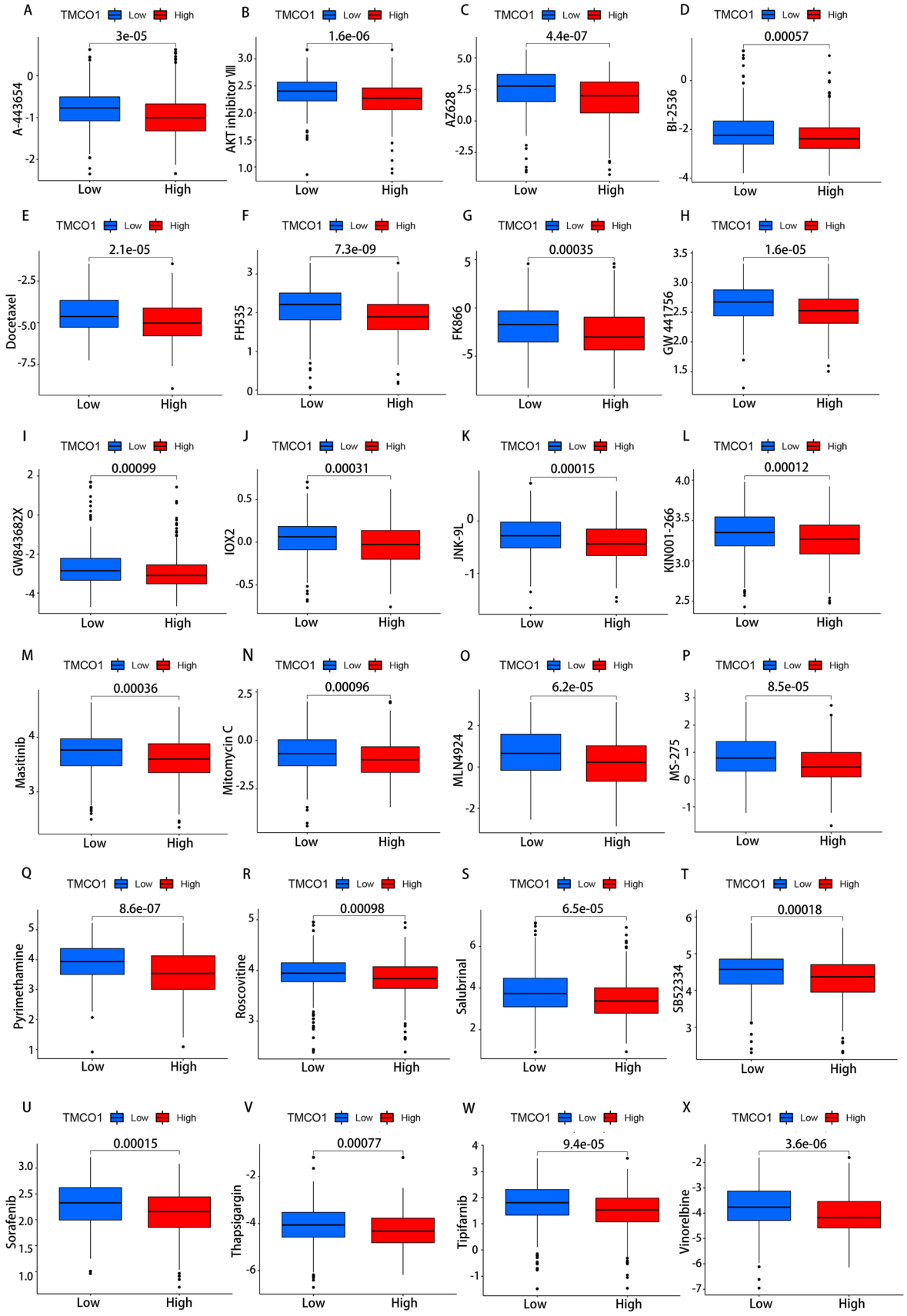

Fig. 7 High expression of TMCO1 is associated with greater drug sensitivity. **A**–**X** Higher TMCO1 expression was associated with increased sensitivity to these 24 drugs in HNSCC patients from the TCGA cohort. $P < 0.05$

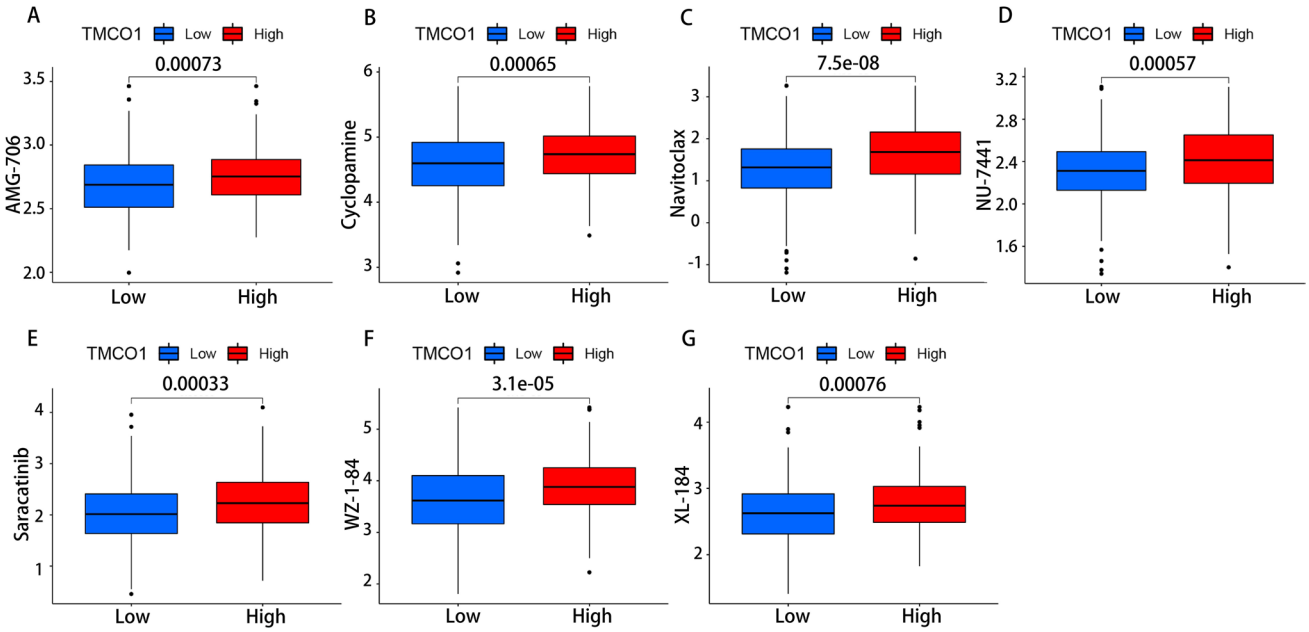

Fig. 8 Low expression of TMCO1 is associated with greater drug sensitivity. **A**–**G** Lower TMCO1 expression was associated with increased sensitivity to these 7 drugs in HNSCC patients from the TCGA cohort. $P < 0.05$

diverse cohorts. These findings deepen the understanding of TMCO1's tissue-specific roles and its potential as a prognostic marker and therapeutic target in HNSCC, paving the way for future mechanistic and translational studies.

In HNSCC, the TMCO1 high-expression group exhibited significant enrichment in keratinization-related pathways (e.g., keratinization, keratinocyte differentiation, and keratin filament) and ion channel activity (e.g., chloride channels and membrane exchange). Keratinization, a hallmark of poor prognosis in HNSCC, OSCC [20], and the enrichment of keratinocyte differentiation and keratin filament pathways in OSCC and oral lichen planus with carcinogenic potential [21], suggest a critical role for TMCO1 in tumor progression. While the precise involvement of TMCO1 in precancerous lesions remains to be fully elucidated, its established role in calcium homeostasis and cellular stress responses hints at a potential contribution to early carcinogenesis, warranting further mechanistic exploration. Notably, chloride channels, which regulate cell volume and membrane potential and are activated by Ca^{2+} [22], may be modulated by TMCO1, given its function as a Ca^{2+} selective cation channel, offering a plausible mechanism for its oncogenic activity.

KEGG enrichment analysis further revealed that TMCO1 regulates extracellular matrix adhesion and tumor metastasis, while GO analysis highlighted its association with keratin filaments, intermediate filaments, and the intermediate filament cytoskeleton, all of which are critical for epithelial cell migration and the transformation of keratinocytes into malignant cells, including squamous cell carcinoma [23]. These findings underscore TMCO1's multifaceted role in driving tumor metastasis and its potential as a therapeutic target in HNSCC, providing a deeper understanding of its molecular mechanisms and paving the way for future translational research.

Immunotherapy has emerged as a pivotal strategy in the treatment of HNSCC yet a significant proportion of patients remain unresponsive to PD-1/PD-L1-based therapies [24]. Our findings revealed that low TMCO1 expression is associated with enhanced anti-PD-1 efficacy but not with anti-CTLA4 response, suggesting that TMCO1 may serve as a predictive biomarker for anti-PD-1 immunotherapy in HNSCC. This aligns with the observation by Li et al., who demonstrated that TMCO1 negatively correlates with tumor-infiltrating CD8 (+) T cells, which are crucial for anti-tumor immunity [19, 25]. Furthermore, TMCO1 expression was inversely associated with M1 macrophages, known for their anti-tumor properties [26], highlighting its potential role in remodeling the TME and influencing immune evasion mechanisms.

Platinum-based chemotherapy remains the cornerstone of first-line treatment for HNSCC, offering tumor shrinkage, stage reduction, and surgical feasibility, particularly for tumors in functionally critical sites [27]. However, chemoresistance poses a significant challenge, limiting therapeutic outcomes. Our KEGG analysis identified TMCO1's involvement in platinum resistance, tyrosine metabolism, and glutathione metabolism, consistent with previous studies. Notably, ongoing phase I and II trials exploring multi-target tyrosine kinase inhibitors in HNSCC aim to overcome resistance pathways and enhance treatment efficacy [28]. Additionally, elevated glutathione levels in LSCC have been shown

to protect cancer cells from chemotherapy [29], further underscoring TMCO1's potential role in chemoresistance. Through drug sensitivity analysis, we identified several chemotherapeutic agents, targeted drugs, and small molecules associated with TMCO1, offering new avenues for biomarker-guided therapy selection and the optimization of anti-tumor immunotherapy. These insights not only deepen the understanding of TMCO1's multifaceted role in HNSCC but also provide a foundation for developing personalized therapeutic strategies to improve patient outcomes.

This study has several limitations that warrant consideration. First, while bioinformatics analysis and in vitro experiments elucidated the functional role of TMCO1 in HNSCC, its precise regulatory mechanisms within the TME, particularly its interactions with immune cells such as CD8 (+) T cells and M1 macrophages, require further validation through in vivo studies. Second, the role of TMCO1 in early carcinogenesis and precancerous lesions of HNSCC remains incompletely understood, and its potential involvement in calcium homeostasis and cellular stress responses merits deeper investigation. Third, the reliance on public databases and the limited sample size may introduce selection bias, necessitating validation with multi-center clinical cohorts and long-term follow-up data to enhance the generalizability of the findings. Finally, the molecular mechanisms underlying TMCO1's association with platinum-based chemotherapy resistance remain unclear, requiring functional experiments and drug screening to confirm its potential as a biomarker for chemoresistance. Addressing these limitations will provide a more comprehensive understanding of TMCO1's biological significance and therapeutic potential in HNSCC.

5 Conclusion

This study provided a comprehensive analysis of TMCO1 in HNSCC, demonstrating its significant overexpression and pivotal role as a potential biomarker and therapeutic target. TMCO1 is strongly associated with poor prognosis and aggressive cancer phenotypes, with its primary function centered on regulating tumor metastasis rather than exerting an equal influence on all aspects of tumor progression. Specifically, TMCO1 promotes cell-ECM adhesion, enhances migratory and invasive capabilities, and supports cell proliferation and survival, thereby driving the malignant progression of HNSCC. Furthermore, low TMCO1 expression correlates with improved response to anti-PD-1 immunotherapy, highlighting its potential in guiding immunotherapeutic strategies. These findings not only deepen the understanding of TMCO1's oncogenic mechanisms in HNSCC but also underscore its therapeutic relevance in targeting tumor metastasis and modulating the immune microenvironment. This study lays a solid foundation for future investigations into TMCO1 as a promising therapeutic target in HNSCC.

Acknowledgements We thank all who made contributions to the manuscript.

Author contributions TL and LC performed literature search, conducted cellular function experiments and drafted the manuscript, figures and tables; GZ, YD and MZ assisted in some of the cellular function experiments; MY, SD and KX analyzed part of the data; SY and HH designed concept of the study and revised the whole manuscript, and obtained the funding. All authors have read and agreed to the published version of the manuscript.

Funding This study was supported by the Research Project of the Heilongjiang Province Health Commission (No. 2019-057), China Primary Health Care Foundation (2022/2023-001) and the Haiyan Scientific Research Fund of Harbin Medical University Cancer Hospital (No. JJMS2021-16).

Data availability Data is provided within the manuscript or supplementary information files.

Declarations

Ethics approval and consent to participate The study was approved by the Ethics Committee of Harbin Medical University Cancer Hospital. All experiments involving human participants were conducted in strict accordance with the Ethical Review Measures for Biomedical Research Involving Human Subjects and relevant guidelines and regulations. Written informed consent was obtained from all participants, confirming their voluntary participation in the study. We have carefully reviewed our methodology section to align with these guidelines, ensuring transparency and reproducibility.

Competing interests The authors declare no competing interests.

References

1. Takeuchi T, et al. Insight toward the MicroRNA profiling of laryngeal cancers: biological role and clinical impact. Int J Mol Sci. 2020;21(10):3693. https://doi.org/10.3390/ijms21103693.
2. Yilmaz E, et al. Immunotherapy and biomarker testing in recurrent and metastatic head and neck cancers: ASCO Guideline. J Clin Oncol. 2023;41(5):1132–46.
3. Cristina V, et al. Immunotherapies and future combination strategies for head and neck squamous cell carcinoma. Int J Mol Sci. 2019;20(21):5399. https://doi.org/10.3390/ijms20215399.
4. Johnson D, et al. Head and neck squamous cell carcinoma. Nat Rev Dis Primers. 2020;6(1):92.
5. Leeman J, et al. Patterns of treatment failure and postrecurrence outcomes among patients with locally advanced head and neck squamous cell carcinoma after chemoradiotherapy using modern radiation techniques. JAMA Oncol. 2017;3(11):1487–94.
6. Ionna F, et al. Recurrent/metastatic squamous cell carcinoma of the head and neck: a big and intriguing challenge which may be resolved by integrated treatments combining locoregional and systemic therapies. Cancers. 2021. https://doi.org/10.3390/cancers13102371.
7. Kozłowska J, et al. Long intergenic non-coding RNAs in HNSCC: from "Junk DNA" to important prognostic factor. Cancers. 2021. https://doi.org/10.3390/cancers13122949.
8. Li T, et al. Exosomes: potential biomarkers and functions in head and neck squamous cell carcinoma. Front Mol Biosci. 2022;9: 881794.
9. Fan H, Shen Y, Yuan Y. Expression and prognostic roles of TRPV5 and TRPV6 in non-small cell lung cancer after curative resection. Asian Pac J Cancer Prev APJCP. 2014;15(6):2559–63.
10. Roderick H, Cook S. Ca2+ signalling checkpoints in cancer: remodelling Ca2+ for cancer cell proliferation and survival. Nat Rev Cancer. 2008;8(5):361–75.
11. Prevarskaya N, Skryma R, Shuba Y. Calcium in tumour metastasis: new roles for known actors. Nat Rev Cancer. 2011;11(8):609–18.
12. Zheng S, et al. iASPP suppresses Gp78-mediated TMCO1 degradation to maintain Ca homeostasis and control tumor growth and drug resistance. Proc Natl Acad Sci USA. 2022. https://doi.org/10.1073/pnas.2111380119.
13. Yang C, et al. Mechanism of transmembrane and coiled-coil domain 1 in the regulation of proliferation and migration of A549 cells. Oncol Lett. 2020;20(5):159.
14. Wang Q, et al. TMCO1 is an ER Ca(2+) load-activated Ca(2+) channel. Cell. 2016;165(6):1454–66.
15. Li C, et al. Transmembrane and coiled-coil domain 1 impairs the AKT signaling pathway in urinary bladder urothelial carcinoma: a characterization of a tumor suppressor. Clin Cancer Res. 2017;23(24):7650–63.
16. Gao L, et al. TMCO1 expression promotes cell proliferation and induces epithelial-mesenchymal transformation in human gliomas. Med Oncol (Northwood, London, England). 2022;39(5):90.
17. Chandrashekar D et al. UALCAN: An update to the integrated cancer data analysis platform. Neoplasia (New York, N.Y.), 2022. 25: 18–27.
18. Lánczky A, Győrffy B. Web-based survival analysis tool tailored for medical research (KMplot): development and implementation. J Med Internet Res. 2021;23(7): e27633.
19. Li H, et al. Screening of tumor antigens and construction of immune subtypes for mRNA vaccine development in head and neck squamous cell carcinoma. Biomolecules. 2022. https://doi.org/10.3390/biom13010090.
20 Cooper T, et al. Association of keratinization with 5-year disease-specific survival in oropharyngeal squamous cell carcinoma. JAMA Otolaryngol Head Neck Surg. 2015;141(3):250–6.
21. Shaw J, et al. Novel sphingolipid-based cancer therapeutics in the personalized medicine era. Adv Cancer Res. 2018;140:327–66.
22. Okuyama K, Yanamoto S. TMEM16A as a potential treatment target for head and neck cancer. J Exp Clin Cancer Res CR. 2022;41(1):196.
23. Velez-delValle C, et al. Epithelial cell migration requires the interaction between the vimentin and keratin intermediate filaments. Sci Rep. 2016;6:24389.
24. Harjunpää H, et al. Cell adhesion molecules and their roles and regulation in the immune and tumor microenvironment. Front Immunol. 2019;10:1078.
25. Ming R, et al. The prognostic signature of head and neck squamous cell carcinoma constructed by immune-related RNA-binding proteins. Front Oncol. 2022;12: 795781.
26. Zhang X, Ji L, Li M. Control of tumor-associated macrophage responses by nutrient acquisition and metabolism. Immunity. 2023;56(1):14–31.
27. Wang J, et al. Identification of several senescence-associated genes signature in head and neck squamous cell carcinoma. J Clin Lab Anal. 2022;36(7): e24555.
28. Sola A, Johnson D, Grandis J. Investigational multitargeted kinase inhibitors in development for head and neck neoplasms. Expert Opin Investig Drugs. 2019;28(4):351–63.
29. Bansal A, Simon M. Glutathione metabolism in cancer progression and treatment resistance. J Cell Biol. 2018;217(7):2291–8.